Journal of Sound and Vibration (2000) **229**(3), 647–667
doi:10.1006/jsvi.1999.2514, available online at http://www.idealibrary.com on IDEAL®

DAMAGE DETECTION USING OUTLIER ANALYSIS

K. WORDEN AND G. MANSON

*Department of Mechanical Engineering, University of Sheffield, Mappin Street, Sheffield S*1 3*JD, England*

AND

N. R. J. FIELLER

*School of Mathematics and Statistics, University of Sheffield, Mappin Street, Sheffield S*1 3*JD, England*

(*Received* 17 *March* 1999, *and in final form* 4 *August* 1999)

This paper constitutes a study of a statistical method for damage detection. The lowest level of fault detection is considered so that the methods are simply required to signal deviations from normal condition; i.e., the problem is one of novelty detection. In this paper, the concept of discordancy from the statistical discipline of outlier analysis is used to signal deviance from the norm. The method is demonstrated on four case studies of engineering interest: one simulation, two pseudo-experimental and one experimental.

1. INTRODUCTION

The problem of damage detection and identification has a natural hierarchical structure. At the higher levels, one might require the diagnostic to return say, information about the expected time to failure of a structure, while at the lowest level, the question is simply of whether a fault is present or not. In many ways, the latter is the most fundamental. In response to the need for robust low-level damage detection strategies, the discipline of *novelty detection* has recently evolved [1, 2]. The problem is simply to identify from measured data if a machine or structure has deviated from normal condition, i.e., if the data is novel. The idea of novelty detection is not entirely new, in many ways the philosophy is coincident with that of classical condition monitoring [3]. However, the new terminology is justified by the fact that novelty detection provides a unifying framework for techniques from a wide range of disciplines. Of the many approaches to the problem, some are drawn from condition monitoring, others from the field of pattern recognition and yet others from multivariate statistics. The latter field has a very substantial body of theory to support it and is proving to be a fruitful source of algorithms for damage detection.

The object of this study is to examine a technique from multivariate statistics and benchmark it on some structures of engineering interest, which have been examined

0022-460X/00/030647 + 21 $35.00/0

by other means elsewhere [4–6]. The method is that of *outlier analysis*. This is a well-established field of statistics which has not yet been systematically exploited for damage detection purposes [7]. It will be shown, that the method not only allows a diagnosis of novelty, but also suggests how the dimension of the data set might be reduced without losing efficiency of the diagnostic.

The structure of the paper is as follows: the following section constitutes a brief tutorial of the relevant theory, this is simply included to make the paper self-contained. The later sections of the paper discuss a number of case studies—from simulation and experiment—of engineering interest.

2. DETECTION AND DISPLAY OF OUTLIERS IN DATA

2.1. OUTLIERS IN UNIVARIATE DATA

A discordant outlier in a data set is an observation that appears inconsistent with the rest of the data and therefore is believed to be generated by an alternate mechanism to the other data. The discordancy of the candidate outlier is a measure which may be compared against some objective criterion allowing the outlier to be judged to be statistically likely or unlikely to have come from the assumed generating model.

In the case of univariate data, the detection of outliers is a relatively straightforward process in that the outliers protrude from one or other end of the data set. There are numerous discordancy tests but one of the most common, and the one whose extension to multivariate data will be employed later, is based on deviation statistics and given by,

$$z_\zeta = \frac{|x_\zeta - \bar{x}|}{s}, \tag{1}$$

where x_ζ is the measurement corresponding to the potential outlier and $\bar{x}$ and s the mean and standard deviation of the sample respectively. The latter two values may be calculated with or without the potential outlier in the sample depending upon whether inclusive or exclusive measures are preferred. This discordancy value is then compared to some threshold value and the observation declared, or not, to be an outlier.

2.2. OUTLIERS IN MULTIVARIATE DATA

A multivariate data set consisting of n observations in p variables may be represented as n points in p-dimensional object space. It becomes clear that detection of outliers in multivariate data is more difficult than the univariate situation due to the potential outlier having the ability to appear more hidden in the data mass. That said, many of the ideas and techniques associated with the detection of outliers in multivariate data follow on from those applicable to univariate problems.

The discordancy test which is the multivariate equivalent of equation (1) is the Mahalanobis squared distance measure given by

$$D_\zeta = (\{\mathbf{x}_\zeta\} - \{\bar{\mathbf{x}}\})^{\mathrm{T}}[\mathbf{S}]^{-1}(\{\mathbf{x}_\zeta\} - \{\bar{\mathbf{x}}\}), \tag{2}$$

where $\{\mathbf{x}_\zeta\}$ is the potential outlier datum, $\{\bar{\mathbf{x}}\}$ is the mean vector of the sample observations and $[\mathbf{S}]$ the sample covariance matrix. T indicates transpose.

As with the univariate discordancy test, the mean and covariance may be inclusive or exclusive measures. In many practical situations the outlier is not known beforehand and so the test would necessarily be conducted inclusively. The outlier displaying component method which is discussed shortly is also an inclusive method. In our case studies however, the potential outlier is always known beforehand and so it is more sensible to calculate a value for the Mahalanobis squared distance without this observation "contaminating" the statistics of the normal data. Whichever method is used, the Mahalanobis squared distance of the potential outlier is checked against an appropriate threshold value, as in the univariate case, and its status determined.

2.3. OUTLIER DISPLAYING COMPONENTS

In order to display multivariate outliers when dealing with data of greater than two or three dimensions it is necessary to apply special graphical methods. Although there are many graphical techniques for multivariate data, most are not specifically designed to display outliers. There is however a graphical method based on Wilks' one-outlier statistic which minimizes the ratio of simplex volumes $|[\mathbf{A}_\zeta]|/|[\mathbf{A}]|$ to highlight the most outlying observation in a data set. $[\mathbf{A}]$ is the matrix of sum of squares and cross-products and $[\mathbf{A}_\zeta]$ the corresponding matrix when the observation being tested, x_ζ, is removed from the sample. This can be shown [8] to be equivalent to being based on the Mahalanobis squared distance measure with the potential outlier included in the calculation of the sample statistics.

The aim is to find a one-dimensional representation of the sample observations so as to highlight the potential outlier x_ζ. The projection vector or one-outlier displaying component, β, which results in the outlier protruding as far as possible from the data mass can be shown [8] to be given by

$$\{\boldsymbol{\beta}\} = [\mathbf{S}]^{-1}(\{\mathbf{x}_\zeta\} - \{\bar{\mathbf{x}}\}), \tag{3}$$

where $[\mathbf{S}]$ and $\{\bar{\mathbf{x}}\}$ denote the covariance matrix and the mean of all the observations respectively. It is then possible to project the original p-dimensional sample $\{\{x_i\}, i = 1, \ldots, n\}$ into the one-dimensional sample $\{y_i, i = 1, \ldots, n\}$ using the one-outlier displaying component so that each y_i is obtained from

$$y_i = (\{\mathbf{x}_i\} - \{\bar{\mathbf{x}}\})^{\mathrm{T}}[\mathbf{S}]^{-1}(\{\mathbf{x}_\zeta\} - \{\bar{\mathbf{x}}\}). \tag{4}$$

Note that y_ζ is equal to the Mahalanobis squares distance of x_ζ from the mean and the other y_i are the values against which y_ζ can be evaluated.

Gordor [8] stated that one of the useful features of the outlier displaying component is its ability to show which dimensions contribute most to the

discordancy of the outlier. It was claimed that the coefficients in the outlier displaying component with the largest absolute values correspond directly to the variables which have the greatest effect on the discordancy. Although it was found to be of some use, a more useful measure of which variables contribute most to the discordancy of an outlier is that of the individual components which sum to give the inclusive or exclusive Mahalanobis squared distances for that outlier. This will be demonstrated later in the case studies.

2.4. CALCULATION OF CRITICAL VALUES OF DISCORDANCY

In order to label an observation as an outlier or an inlier there needs to be some threshold value against which the discordancy value can be compared. This value is dependent on both the number of observations and the number of dimensions of the problem being studied. The value also depends upon whether an inclusive or exclusive threshold is required.

A Monte Carlo method was used to arrive at the threshold value and this may be summarized by the following steps.

(1) Construct a $(p \times n)$ (number of dimensions $\times$ number of observations) matrix with each element being a randomly generated number from a zero mean and unit standard deviation normal distribution. For the first case study in the following section this would mean constructing a (50×1000) matrix to represent the normal condition set of 1000 observations of dimension 50.
(2) Mahalanobis squared distances calculated for all the observations, using equation (2) where $\{\bar{\mathbf{x}}\}$ and $[\mathbf{S}]$ are either inclusive or exclusive measures (depending on the type of threshold being conducted), and the largest value stored. For the first case study, the largest of the 1000 Mahalanobis distances would be stored.
(3) Process repeated for a large number of trials whereupon the array containing all the largest Mahalanobis squared distances then ordered in terms of magnitude. The critical values for 5 and 1% tests of discordancy for a p-dimensional sample of n observations are then given by the Mahalanobis squared distances in the array above which 5 and 1% of the trials occur.

3. CASE STUDIES

This section applies the theory outlined above to four systems of engineering interest. The first data set is simulated whilst the second and third are *pseudo-experimental* in that they are based on measured data with an expected level of measurement noise added to result in a larger set of normal (unfaulted) data. The final data set is entirely experimental.

3.1. A SIMULATED STRUCTURE

The simulated system which was tested in order to demonstrate the Mahalanobis squared distance method of detecting outliers and to test the methods which

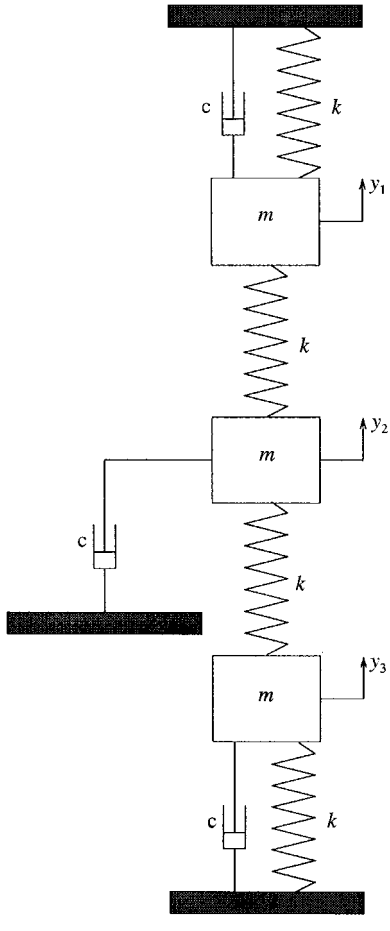

Figure 1. The three-degree-of-freedom simulated system.

indicate the dimensions of high contribution to the outlier discordancy value was the three-degree-of-freedom (3-d.o.f.) lumped-parameter system shown in Figure 1. The equations of motion of this system are

$$m\ddot{y}_1 + c\dot{y}_1 + 2ky_1 - ky_2 = x_1(t),$$

$$m\ddot{y}_2 + c\dot{y}_2 - ky_1 + 2ky_2 - ky_3 = x_2(t),$$

$$m\ddot{y}_3 + c\dot{y}_3 - ky_2 + 2ky_3 = x_3(t) \tag{5}$$

The values $m = 1$, $c = 20$, and $k = 10^4$ were used for the unfaulted condition.

The feature which was used for the detection process was the transmissibility function between masses 1 and 2. This has previously proved useful in pattern recognition for vibration problems [9]. It was computed by simulating the response to a harmonic excitation $x_1(t) = X\cos(\omega t)$ for a frequency range between 0 and 50 Hz. The relative gain and phase between y_1 and y_2 was extracted in each case. However, only the magnitude was used for the process. The transmissibility

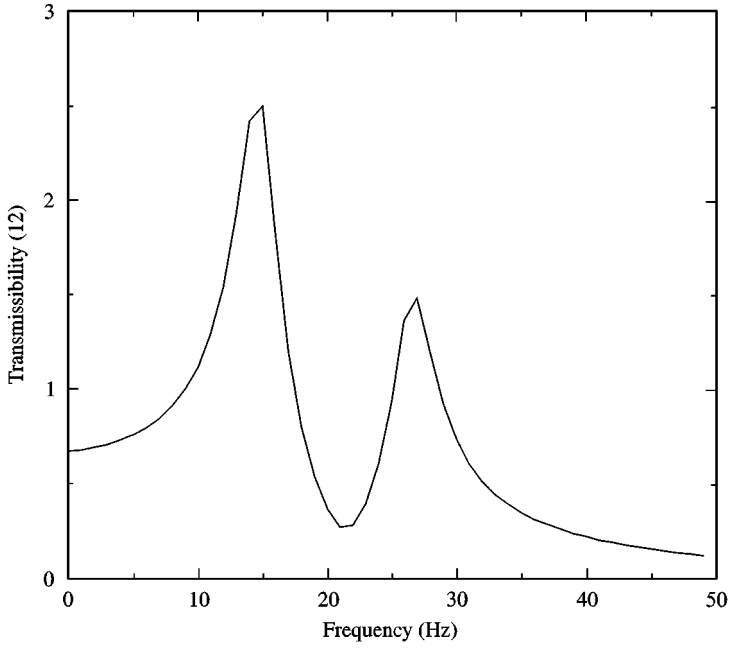

Figure 2. Transmissibility function for the unfaulted data.

function was sampled at 50 regularly spaced points on the frequency range to give the pattern to be used as the unfaulted condition in the analysis. This pattern is shown in Figure 2.

The fault in this system was simulated by reducing the stiffness between masses 1 and 2 by 1, 10 and 50% of the original value and the three faulted patterns were calculated in the same manner as above with the stiffness altered in the equations of motion.

In order to construct a suitable mean vector $\{\bar{\mathbf{x}}\}$ and a covariance matrix $[\mathbf{S}]$, for the normal condition, the unfaulted pattern was copied 1000 times and each copy was subsequently corrupted with different Gaussian noise vectors of r.m.s. 0·05. The three testing patterns were also copied 1000 times each and corrupted with the same noise level. These three data sets were then concatenated on to the normal data to give a 4000 observation testing data set.

The exclusive Mahalanobis squared distances for each of these 4000 observations were then calculated using equation (2) and the results plotted as shown in Figure 3. The 1% exclusive threshold value for a 1000 observation, 50-dimensional problem was found to be 109 after 1000 trials. The plot shows that the unfaulted data points (first 1000 observations) were all correctly labelled as inliers, as expected, and that all the observations corresponding to the 10 and 50% stiffness reductions (third and fourth sets of 1000 observations respectively) were correctly diagnosed as outliers. Unfortunately, the method is unable to classify any of the 1% reduction observations (second set of 1000 observations) as outliers.

It was stated in the previous section that Gordor [8] suggested that the outlier displaying component may be used to indicate which dimensions contribute most

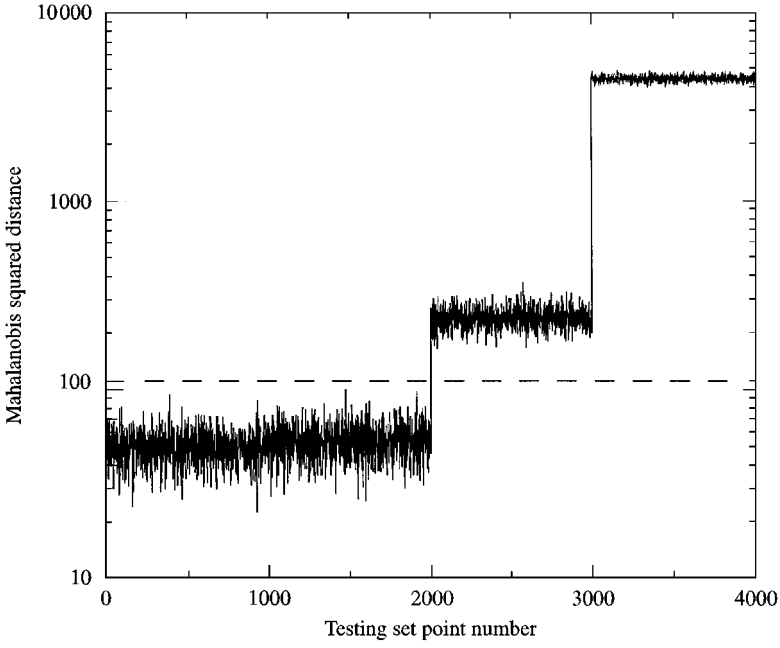

Figure 3. Mahalanobis squared distances for unfaulted and faulted cases. (– – –) Threshold value.

to the discordancy of the outlier. Equation (3) was used to calculate the outlier displaying components for all 1000 of the unfaulted testing observations. The absolute values were then averaged to give a single average outlier displaying component for the unfaulted data. Although we refer to outlier displaying components for the unfaulted data they should merely be thought of as projection vectors which convert p-dimensional observations into a corresponding univariate observation so as to emphasize the particular test observation. This procedure was repeated for the other three sets of 1000 observations corresponding to the three fault conditions to give average outlier displaying components for the 1, 10 and 50% faults and the results are shown in Figure 4. This appears to show that the dimensions with the greatest contribution to the discordancy are those which are near to the two peaks of the transmissibility function of Figure 2. This is not surprising as the greatest effect of stiffness variation would be expected around the resonances. It should be noted that the outlier displaying component values for all dimensions of the unfaulted case are nominally zero.

A similar procedure to that outlined above was conducted to calculate the contributions of the individual dimensions to the overall Mahalanobis squared distance. As the results given in Figure 3 are exclusive measures, the individual contributions will also be based on the data sets with the potential outlier excluded from the mean vector and covariance matrix. To clarify, this method examines the individual components of equation (2) which are summed to give the overall Mahalanobis squared distance for some observation. Figure 5 shows the results for each of the four conditions when averaged over the 1000 observations. This can be seen to produce smoother plots than those of the outlier displaying component

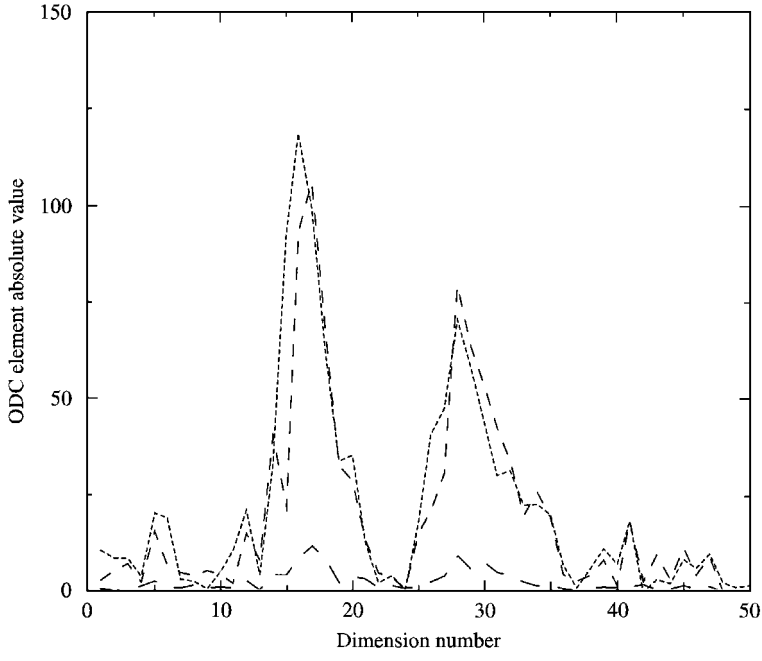

Figure 4. Averaged outlier displaying components. —— No fault; – – – 1% fault; - - - 10% fault; ··· 50% fault.

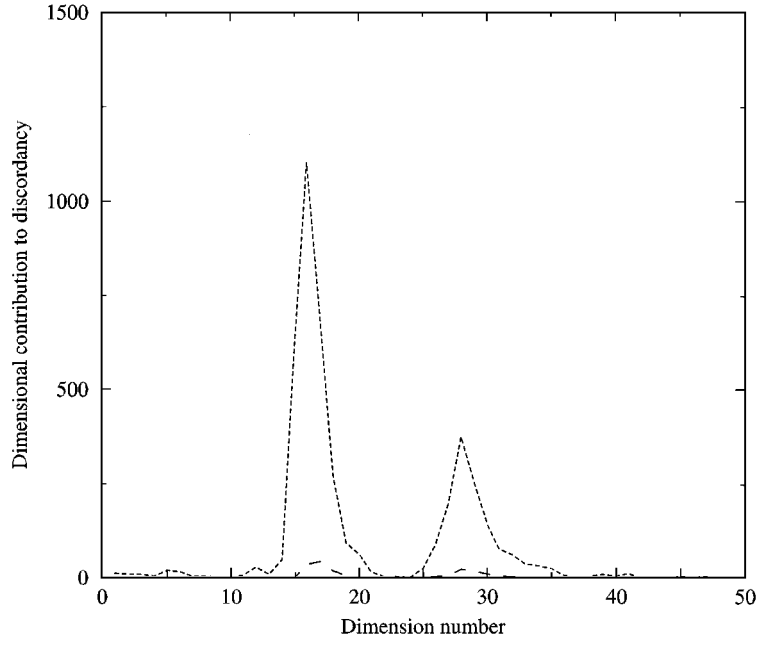

Figure 5. Averaged individual contributions to Mahalanobis squared distance. —— No fault; – – – 1% fault; - - - 10% fault; ··· 50% fault.

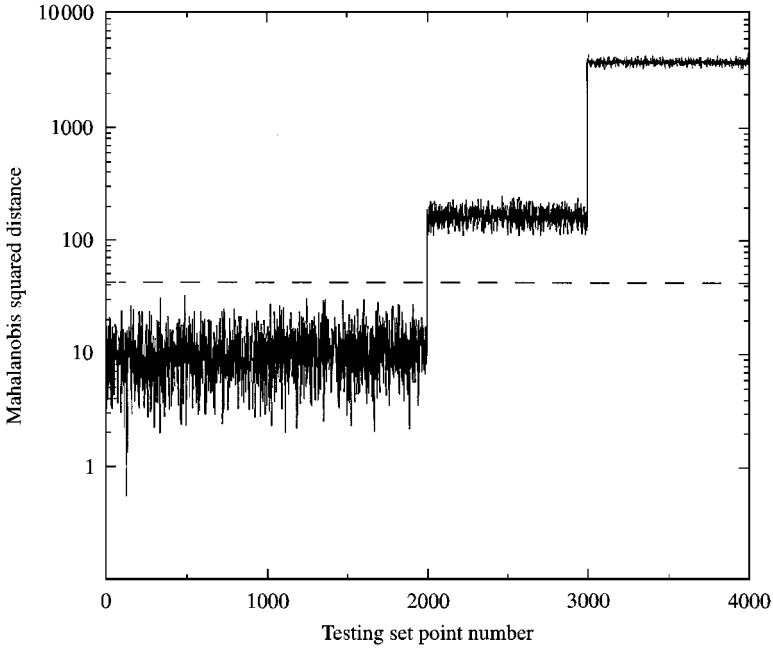

Figure 6. Mahalanobis squared distances for unfaulted and faulted cases for the reduced dimension data. (– – –) Threshold value.

results of Figure 4 and thus give a stronger indication that it may be possible to reduce the number of dimensions of the problem from the original 50 dimensions.

In order to test this idea, the data sets were copied and reduced to contain only the information from dimensions 14–18 inclusive and 26–30 inclusive (i.e., around each of the transmissibility function peaks). The exclusive Mahalanobis squared distances for each of the 4000 observations were then calculated for the 10-dimensional problem using equation (2) and the results plotted in Figure 6. The 1% exclusive threshold value for a 1000 observation, 10-dimensional problem was found to be 43·6 after 1000 trials. The plot shows that this dimensional reduction has no effect on the detection of outliers. Once again, the unfaulted data points were all correctly labelled as inliers and all the 10 and 50% fault observations were correctly identified as outlying. As in the 50-dimensional case, the method was unable to classify any of the observations with 1% stiffness reduction as being an outlier.

This has illustrated that it may be possible to reduce the number of dimensions in a problem by examining the contribution to the outlier discordancy of each dimension thus resulting in a large saving in computational time without a significant loss in classification ability.

3.2. GEARBOX EXPERIMENTAL DATA

The aim of this case study was to try to detect the onset of a local tooth fault in a spur gear. The experimental spur gear vibration data was obtained from a system

comprising a 24-tooth input gear driven by an electric motor and meshing with a 16-tooth pinion. The rotational frequency of the pinion was 37·5 Hz. resulting in a meshing frequency of 600 Hz. The type of failure which was studied was the partial removal of a tooth. This type of failure is a common fault in many industrial applications [10]. The experiment involved five separate fault advancements: the removal of 1 mm depth of a single tooth across 25, 50, 75 and 100% of the tooth facewidth and the same defect with the 100% advancement on two pinion teeth.

Acceleration vibration signals were measured in the horizontal direction at the pinion bearing housing and five meshing harmonics were observed in the power spectra for the unfaulted condition and all five faulted conditions. For the purpose of outlier detection these five harmonics were deemed to contain the most useful information and subsequently three frequency lines were taken about each peak thus reducing the problem to one of 15 dimensions.

The experiment only yielded a single pattern for the unfaulted and each of the faulted conditions. In order to provide a suitable bank of unfaulted data, the unfaulted pattern was copied 1000 times and each was distorted by the addition of a Gaussian noise vector with an r.m.s. set at 5% of the spectral peak magnitude. (Note that this was a subjective decision based on engineering judgement in the absence of sufficient normal condition data. Research is currently underway on methods of estimating the required level of noise corruption for the expansion of the training set.) The object of this exercise is to produce a novelty detector which never fires purely because a measured pattern is noisy. In the absence of any prescription for the noise, the Gaussian process (with unit-proportional covariance matrix) was chosen; a minimal requirement for any pattern recognition system is that it should be transparent to normally distributed noise. In previous paper such data has been referred to as *pseudo-experimental* because, although the basic templates come from experiment, there is not enough data to estimate the real extent and colour of the noise process which shapes the probability density function. This approach is at least a step up from the studies using only simulated data.

Three examples of the corrupted data vectors obtained from the original unfaulted pattern are shown in Figure 7. These 1000 15-dimensional observations were used to calculate a mean vector, $\{\bar{\mathbf{x}}\}$, and a covariance matrix, $[\mathbf{S}]$, for the unfaulted condition. Each of the testing patterns were then introduced in turn and values for the exclusive Mahalanobis squared distance were calculated using equation (2). The threshold value was calculated using the method discussed in the last section. For a 1000 observation, 15-dimensional problem the 1% exclusive threshold value was found to be 50·6 after 1000 trials.

Figure 8 shows the values for each of the six patterns. Not surprisingly, case 1, the unfaulted condition, has a negligible Mahalanobis distance since this pattern was actually used to generate the bank of unfaulted data. All five of the faulted patterns are correctly flagged as outliers. Cases 2–5 correspond to the single tooth fault with 25, 50, 75 and 100% advancement, respectively, with the only surprising result being the drop in Mahalanobis squared distance from the 25% advancement to the 50% advancement. Similarly, surprising but easier explained is the 100% advancement on two teeth data, case 6, having the lowest Mahalanobis squared

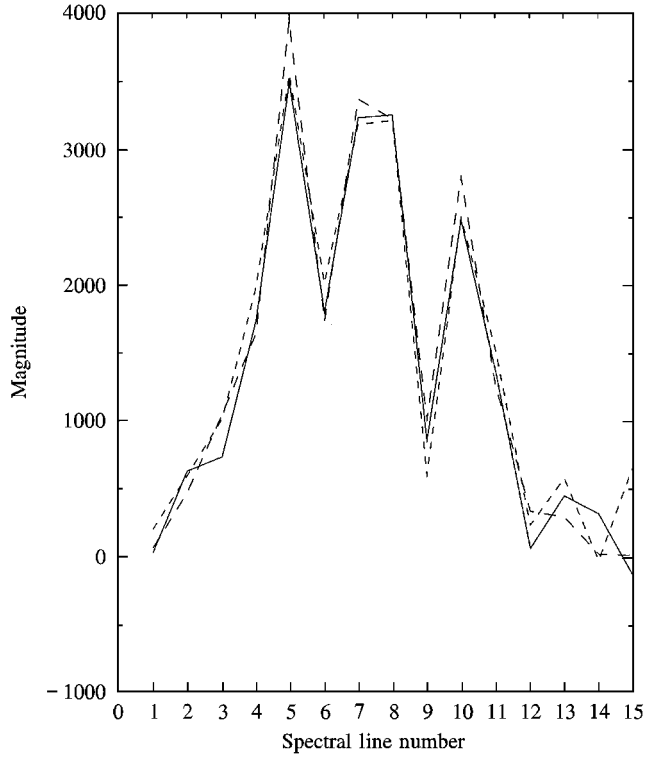

Figure 7. Power spectrum points of interest from the spur gear vibration signals.

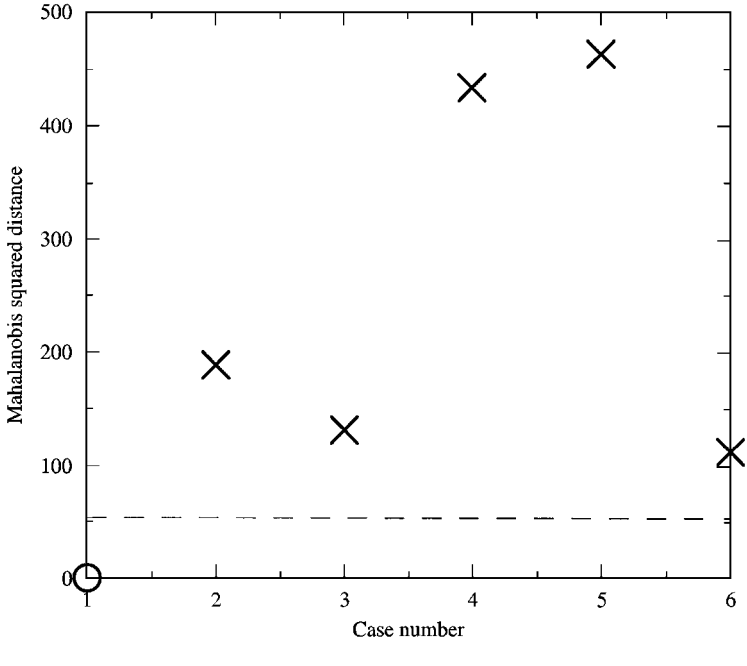

Figure 8. Mahalanobis squared distances for unfaulted (○) and faulted (×) cases. (– – –) Threshold value.

distance of all the faulted cases. This is most likely due to the more intensive modulation processes which occur with the two faulted teeth and result in less energy being transferred to the five meshing harmonics. This could be tested by increasing the number of dimensions of the problem to include measurements from frequency lines between the meshing harmonics.

Dimensional reduction was found not to be possible due to all dimensions contributing significantly to outlier discordancy when examined using the method discussed in the previous case study.

3.3. LAMB-WAVE EXPERIMENTAL DATA

The third case study is the attempt to detect defects in carbon fibre composite plates using ultrasonic Lamb wave data. Two separate plates with differing fault conditions and positions were analyzed. The same procedure was used in each test. This being that fundamental symmetric Lamb waves were launched using a perspex wedge acoustic transducer driven by a 5 cycle toneburst. An optical fibre was embedded (in the case of the first plate) or bonded (in the case of the second) across the full plate width. This fibre was positioned between the source and the known line of defects in order to allow monitoring of the outgoing wave followed by reflections from any defects and the far edge of the plate. Figure 9 shows a typical normalized Lamb wave reflection signal from a defect-free region. The large outgoing pulse and the following backwall reflection may be observed. If there were any defect in the path of the pulse then this would manifest itself in another

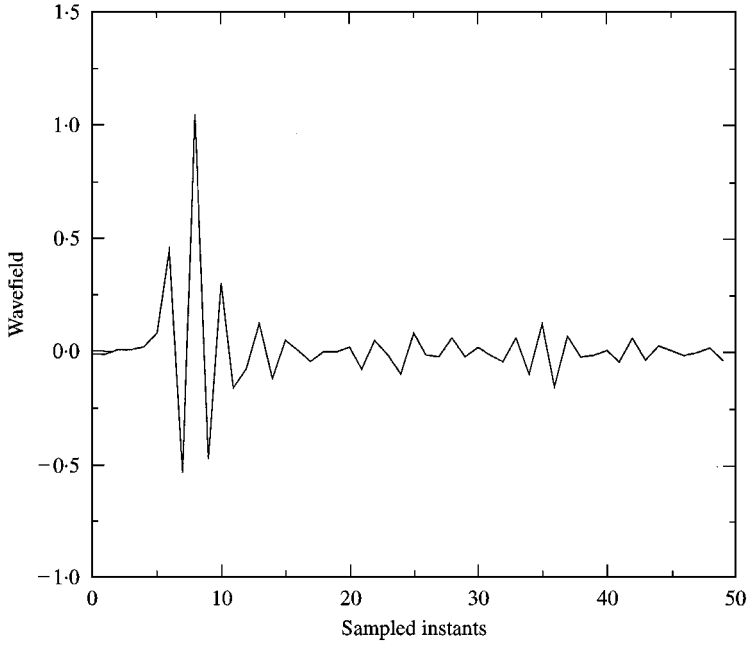

Figure 9. Measured Lamb-wave record (decimated).

reflection seen between the outgoing pulse and the backwall reflection on the time signal. The signals from the optical fibre were monitored by a digital storage oscilloscope and stored on a PC. In each test, readings were taken across the full plate width in 10 mm increments by moving the acoustic source which was driven at a centre frequency of 250 kHz. This frequency, combined with the plate thickness of 3 mm resulted in a frequency-thickness product of less than 1 MHz mm allowing only the fundamental symmetric and antisymmetric modes to propagate. This simplified the testing procedure.

3.3.1. *Plate 1*

An in-depth description of the first set-up is given in reference [6]. Figure 10 shows details of the 3 mm thick carbon fibre plate. The panel incorporated a 20×20 mm square void delamination located at $\frac{1}{4}$ of the plate thickness at a distance of nominally 150 mm from the left-hand edge of the plate.

Seventeen readings were taken at 10 mm intervals across the plate width starting at 70 mm from the left-hand edge of the plate up to 230 mm from this edge. These reflections signals were then decimated to give 50 sampling points for each source position. In order to construct an unfaulted bank of data for the purpose of calculating the mean vector and covariance matrix, the two outermost readings from each side (i.e., readings 1, 2, 16 and 17), which were known to be defect-free, were each copied 250 times and corrupted with different Gaussian noise vectors. The r.m.s. of the noise process was taken as 0·1 giving an imposed signal-to-noise ratio of the order of 10·0. (Note that this was a subjective decision based on

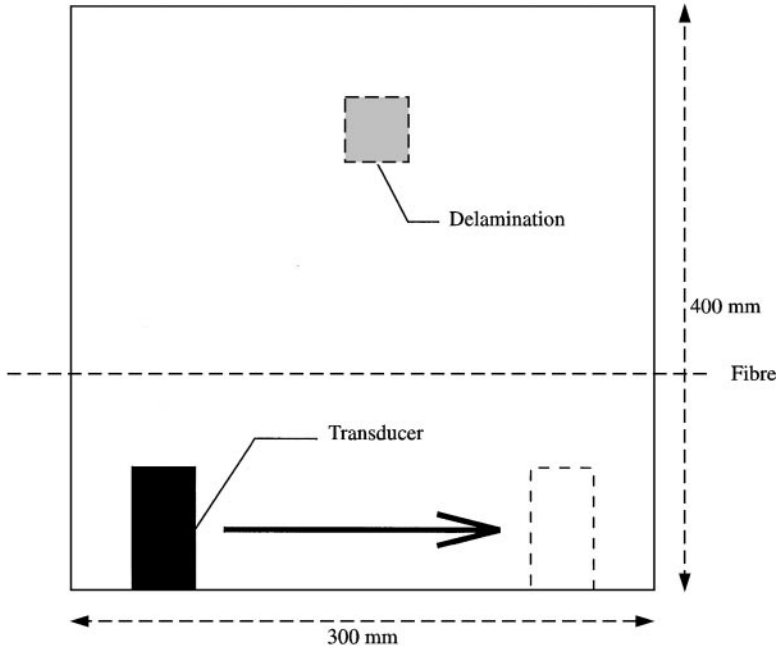

Figure 10. Details of mixed carbon/glass fibre reinforced panel.

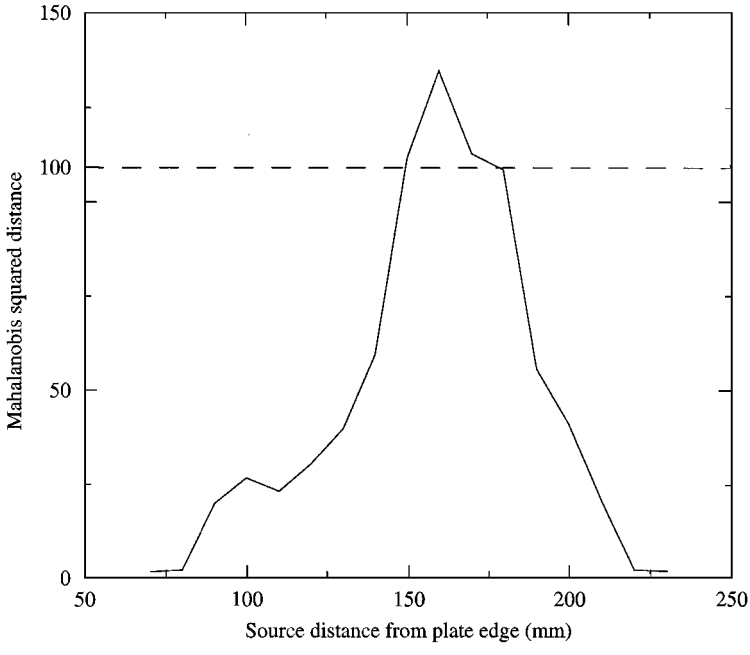

Figure 11. Mahalanobis squared distances for 17 measurement points. (– – –) Threshold value.

engineering judgement in the absence of normal corruption data. Research is currently underway on methods of estimating the required level of noise corruption for the expansion of the training set.) This done, the Mahalanobis squared distances for the 17 sets of testing data were then calculated using equation (2). The results are given in Figure 11. Note that the threshold value is the same as that for the simulated system case study due to the number of dimensions and observations being the same in the two normal data sets. So, the 1% threshold value is again 109. It can be seen that the method flags the measurements from 150 to 170 mm which are in the region of the actual fault as outlying the set of normal data. Allowing for the beam spreading as a results of the finite-width launch transducer, the procedure has also obtained a sensible size estimate for the defect (20 mm $\times$ 20 mm delamination).

3.3.2. *plate* 2

The procedure detailed above was repeated for the second plate with the only difference being that data were only retained from the second and third quarters of the time record. This was to focus on the interval of interest which contained the reflection from the defect. The 3 mm thick plate was 430 mm long by 470 mm wide and incorporated two defects (Figure 12). These defects were a simulated delamination at a distance of 75 mm from the right-hand plate edge and a simulated resin rich area at a distance of 225 mm from the same edge.

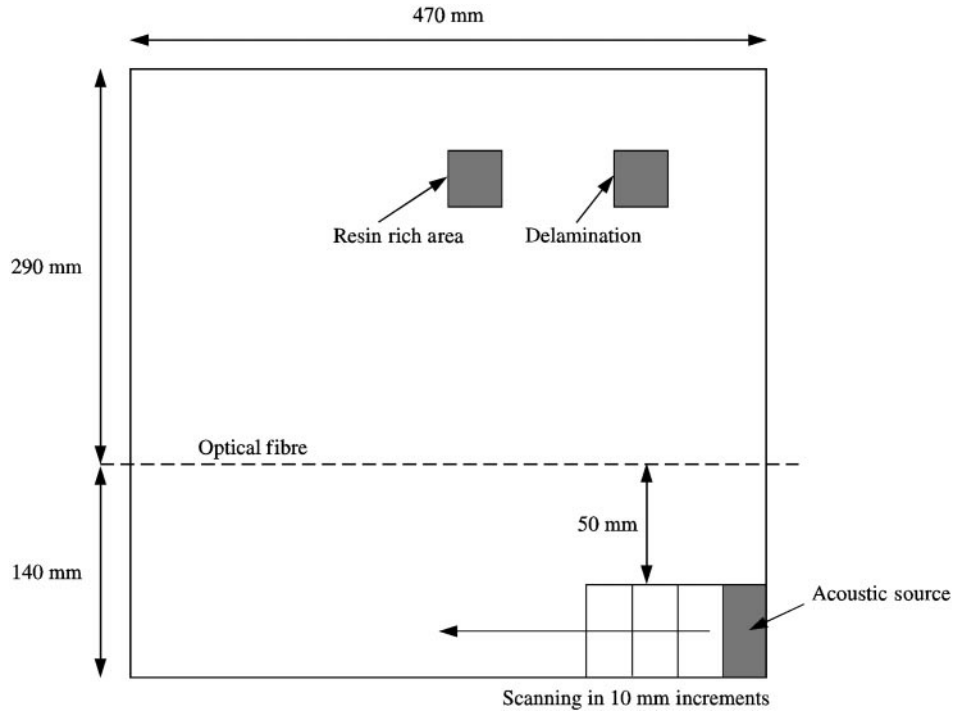

Figure 12. Details of carbon fibre plate with two defects.

Forty-three readings were taken at 10 mm intervals across the plate width starting at 30 mm from the right-hand edge of the plate up to 440 mm from this edge. The resulting signals were decimated to give 50 sampling points for each of the 43 positions. As in the case of the first plate, the two outermost patterns from each side of the plate were taken to represent normal condition and each copied 250 times and corrupted with r.m.s. 0·1 Gaussian noise thus giving a bank of 1000 training points.

The Mahalanobis squared distances for all 43 training points were then calculated using equation (3). Figure 13 shows the results. The two faults are clearly identified. The first is as 70 ± 10 mm (three values were flagged as outlying) which is in excellent agreement with the actual delamination located at 75 mm. One can infer that the delamination extends for about 20 mm as expected. The second fault is indicated at 260 ± 10 mm which shows reasonable agreement with the expected 225 mm. Again the extent of the defect is shown.

As was the case with the gearbox data in the previous case study, it was not possible to use the individual components of the Mahalanobis squared distances to reduce the dimension of the problem in either plate due to the majority of the dimensions having a significant contribution to the overall squared distance.

3.4. BALL-BEARING EXPERIMENTAL DATA

The final case study was concerned with trying to detect various fault conditions within a ball-bearing housing. An introduction to traditional methods of bearing

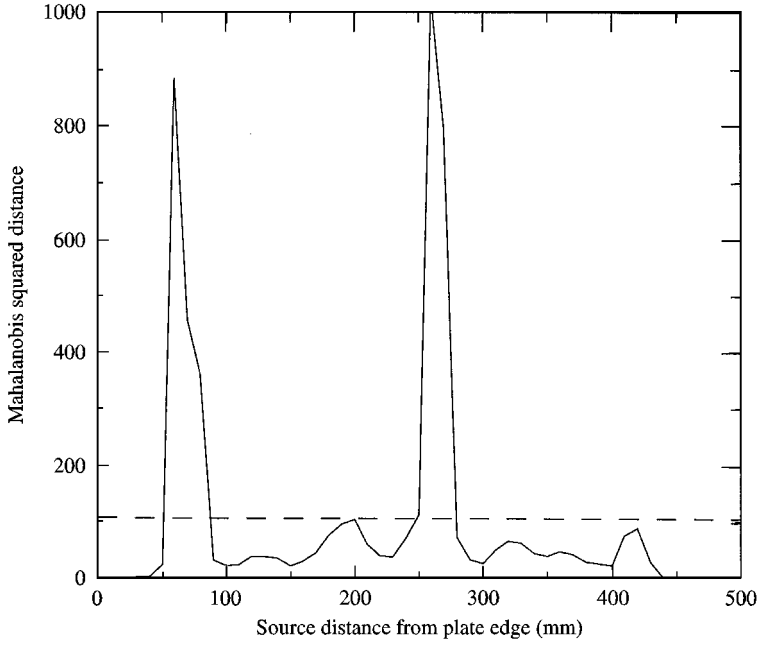

Figure 13. Mahalanobis squared distances for 43 measurement points. (– – –) Threshold value.

monitoring can be found in reference [3]. In this study a loaded shaft supported on two bearings was rotated at 24·6 Hz and acceleration vibration signals acquired from the casing of the test bearing. The four fault conditions which were examined were a completely broken outer race, a broken cage with one loose element, a damaged cage with four loose elements and finally, a badly worn ball-bearing. For the purpose of outlier detection 32 equispaced spectral points were taken from the measured 0–8192 Hz frequency range. Three hundred and eighty four patterns were obtained each condition, including the unfaulted case, except for the broken outer race condition for which only 320 patterns were obtained. Figure 14 shows examples of two power spectral patterns.

This is the first of the four case studies which does not require an artificial bank of unfaulted data to be constructed from only a few patterns distorted by Gaussian noise vectors. The 384 32-dimensional experimental observations were used to calculate the mean vector, $\{\bar{\mathbf{x}}\}$, and the covariance matrix, $[\mathbf{S}]$, for the unfaulted condition. Repeating the same procedure described in the previous case studies, each of the testing patterns were introduced in turn and values for the exclusive Mahalanobis squared distance were calculated using equation (2). The 1% exclusive threshold value for a 384 observation, 32-dimensional problem was found to be 86·8 after 1000 trials.

Figure 15 shows the exclusive Mahalanobis squared distances for all the observations. Testing set points 1–384 represent the unfaulted condition; 385–704, the broken outer race; 705–1088, the one loose element; 1093–1472, the four loose elements and 1473–1856, the worn bearing. It can be seen that all the observations from all four faulted conditions have been correctly labelled as outliers.

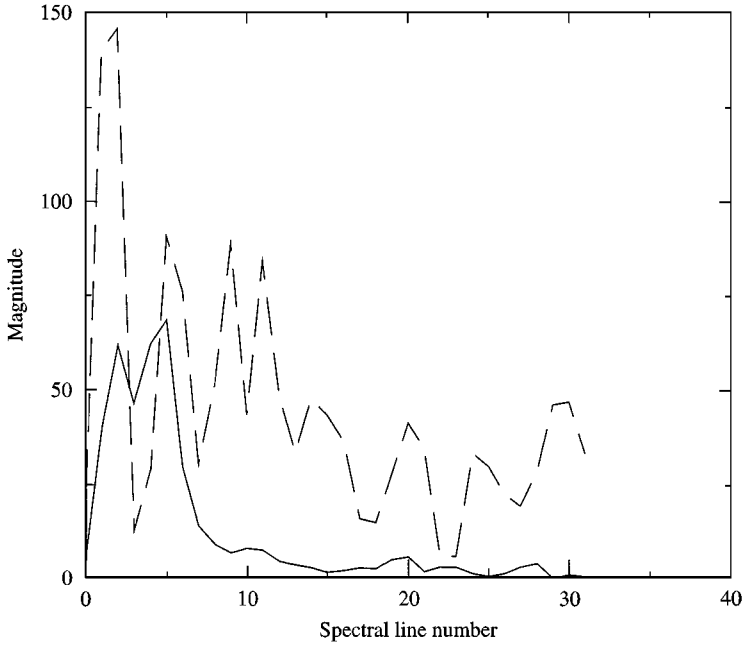

Figure 14. Power spectral patterns from the ball-bearing vibration signals. — Unfaulted; — – broken cage (1 element)

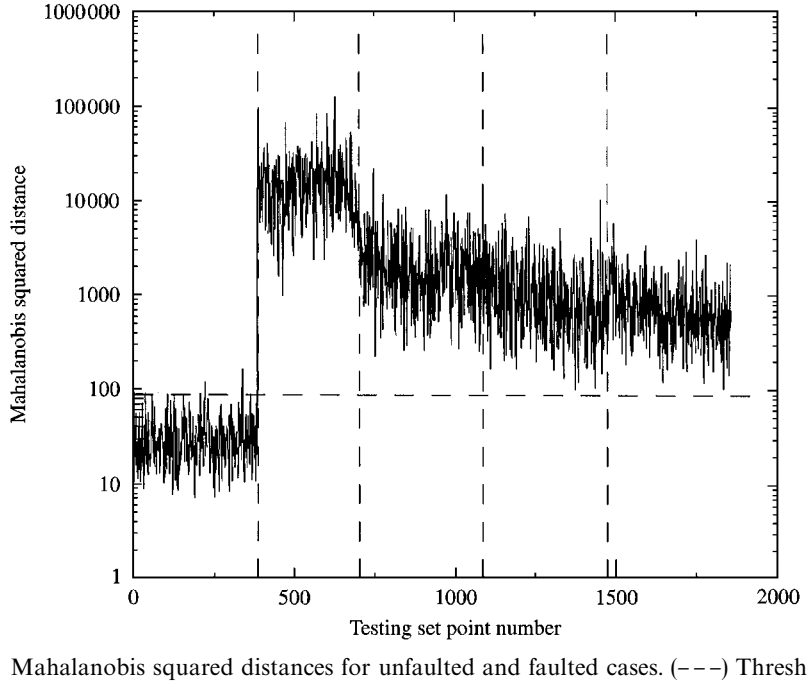

Figure 15. Mahalanobis squared distances for unfaulted and faulted cases. (– – –) Threshold value.

Unfortunately, around 10 of the 384 unfaulted observations have also been flagged as outliers. This is however a preferable situation to that of incorrectly diagnosing an outlying observation and some misclassifications are expected due to the probabilistic nature of the threshold estimation.

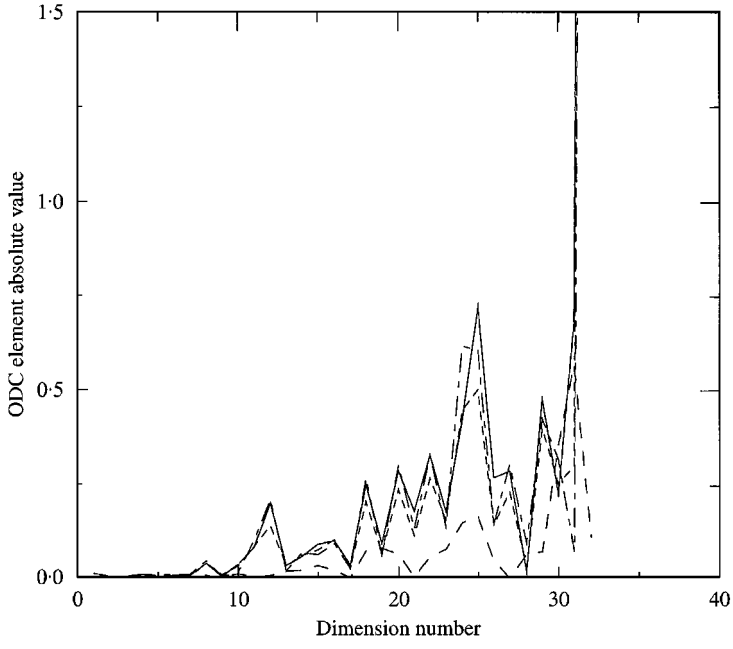

Figure 16. Averaged outlier displaying components. ··· Unfaulted; – – – broken outer race; - - - 1 loose element; — 4 loose elements; —·— Worn bearing

In order to see whether any reduction in the number of dimensions of this problem were possible, the outlier displaying component for each observation was calculated using equation (3). The absolute values were then averaged over the unfaulted and each fault condition to give five average outlier displaying components. Again, when we refer to outlier displaying components for the unfaulted data they should merely be thought of as projection vectors which convert p-dimensional observations into a corresponding univariate observation so as to emphasize the particular test observation. Figure 16 shows the results of this analysis. Although the plot clearly shows that the important dimensions as regards outlier detection are those at the higher end of the frequency range, it seems that approximately half of the dimensions are still of significance to the problem. In order to see whether the contributions to discordancy of the individual dimensions could add anything to the problem, the procedure discussed in the simulated structure case study was repeated for the ball-bearing problem.

As in the simulated structure case study, the individual contributions will also be based on the data sets with the potential outlier excluded from the mean vector and covariance matrix. Figure 17 shows the results for each of the five conditions when averaged over all observations pertaining to that condition. This agrees with the last plot in that the important dimensions are those relating to the higher frequencies. However, this method indicates that it may be possible to reduce the problem from 32 dimensions to only 10 and still produce similar results by considering only the last 10 readings of every observation.

In order to check whether this is the case, the data sets were copied and reduced to contain only the information from dimensions 23–32 inclusive. The exclusive

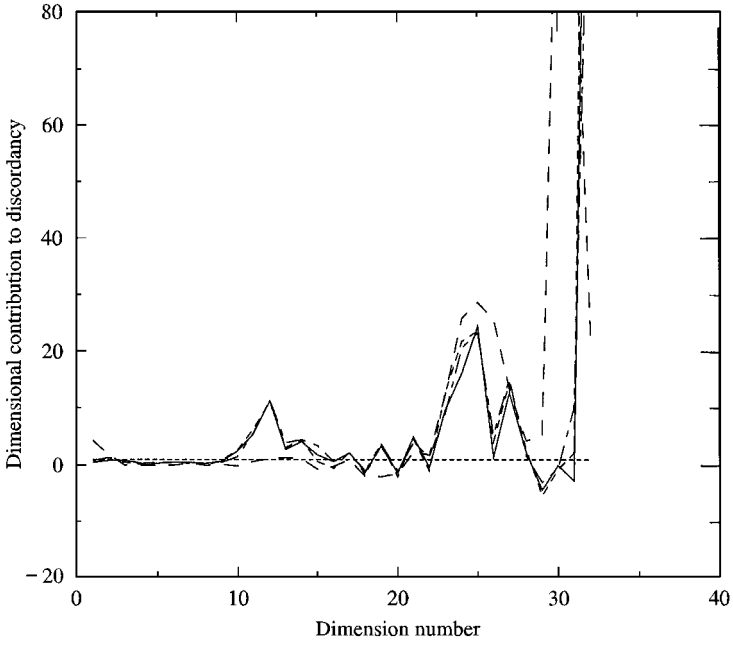

Figure 17. Averaged individual contributions to Mahalanobis squared distance. ··· Unfaulted; – – – broken outer race; - - - 1 loose element; — 4 loose element; ———— Worn bearing

Mahalanobis squared distance for each observation was calculated for the ten-dimensional problem using equation (2) and the results plotted in Figure 18. The 1% exclusive threshold value for a 384 observation, 10-dimensional problem was found to be 40·4 after 1000 trials. The plot appears very similar to that for all 32 dimensions shown in Figure 15. In fact, it has reduced the number of incorrectly labelled unfaulted conditions to only 7 out of 384 but it has failed to designate two of the faulted observations as outliers.

Again, as was the case with the structural case study, it has proved possible to reduce the number of dimensions of the problem without a significant loss in classification ability and with a large saving in computational time.

In order to compare this to Principal Component Analysis, the dimension was also reduced to 10 using this popular method and the exclusive Mahalanobis squared distance was calculated for each observation. Figure 19 gives the results and it can be seen to be a less effective method than that of retaining the largest contributing dimensions to the Mahalanobis squared distances: there are more false positives over the normal condition set and more false negatives over the anomalous measurements.

4. DISCUSSION AND CONCLUSIONS

The methods of outlier analysis, have been adapted to the problem of damage detection. A conceptually simple approach based on Mahalanobis distance has been demonstrated successfully on a number of high-dimensional data sets.

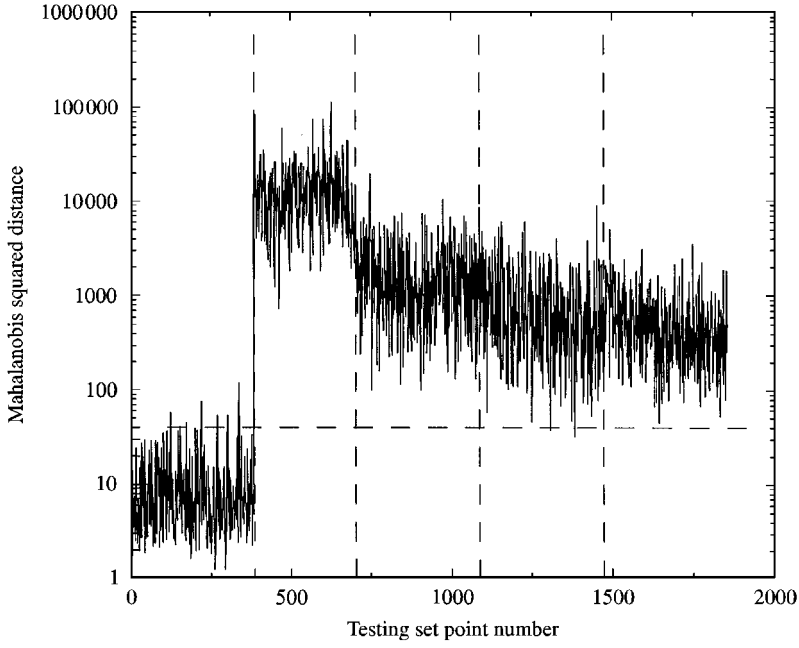

Figure 18. Mahalanobis squared distances for unfaulted and faulted cases for the reduced dimension data. (– – –) Threshold value.

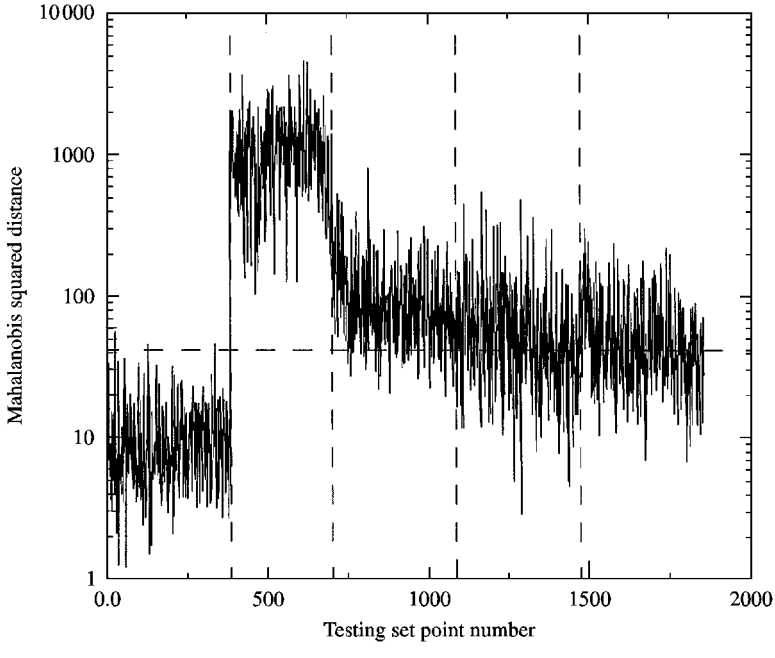

Figure 19. Mahalanobis squared distances for unfaulted and faulted cases for the first ten principal components. (– – –) Threshold value.

However, along the way, a certain number of assumptions have been made. First of all, it is assumed that a single outlier is present. This simplifies the problem enormously as the effects of masking and swamping which plague the problem of multiple-outlier analysis can be ignored. This is justified by an assumption that a data set is available for computing the covariance matrix, etc. which purely contains points corresponding to normal operation. If this is true, subsequent observations can be examined in isolation as they are measured, and further, an exclusive measure can be used.

In choosing the Mahalanobis distance, there is an implicit assumption that the normal condition set has Gaussian statistics. While this is unlikely to give problems if the distribution is near-Gaussian, it will certainly invalidate the approach if there are gross deviations, e.g., if the distribution is multi-modal. In such cases, other techniques can be used such as Kernel Density Estimation.

REFERENCES

1. C. M. Bishop 1994 *IEE Proceedings—Vision and Image Processing* **141**, 217–222. Novelty detection and neural network validation.
2. L. Tarrasenko, P. Hayton, Z. Cerneaz and M. Brady 1995 *Proceedings of fourth IEE International Conference on Artificial Neural Networks*, *Cambridge*, *UK*, *Vol.* 409, 442–447. Novelty detection for the identification of masses in mammograms.
3. C. Cempel 1991 *Vibroacoustic Condition Monitoring*. Chichester: Ellis Horwood.
4. W. J. Staszewski and K. Worden 1996 *Neural Computing and Applications* **5**, 160–183. Classification of faults in gearboxes—pre-processing algorithms and neural networks.
5. K. Worden 1997 *Proceedings of the 15th International Modal Analysis Conference*, *Florida*, 631–637. Damage detection using a novelty measure.
6. W. J. Staszewski, S. G. Pierce, K. Worden, W. R. Philp, G. R. Tomlinson and B. R. Culshaw 1997 *Optical Engineering* **36**, 1877–1888. Wavelet signal processing for enhanced Lamb wave defect detection in composite plates using optical fibre detection.
7. V. Barnett and T. Lewis 1994 *Outliers in Statistical Data*. Chichster: Wiley.
8. B. K. Gordor 1994 *Ph.D. Thesis*, *University of Sheffield*. Some informal methods for the detection and display of outliers in data.
9. Q. Chen, Y. W. Chan, K. Worden and G. R. Tomlinson 1994 *Proceedings of the International Conference on Vibration Engineering*, *Beijing*, *China*, 567–577. Structural fault detection using neural networks trained on transmissibility functions.
10. N. Johnson 1995 *Technical Report Doc.* 155/1163, *Vickers Shipbuilding and Engineering Ltd.*, *Barrow-in-Furness*, *Cumbria*. Gearbox health monitoring—definitions of FZG spur gear seeded fault trials.